Draft Publication; ESRF REPORT,

To be submitted to Thin Solid Films or related journal.

Electroless nanoworm Au films on columnar porous silicon layers.

Alvaro Muñoz-Noval[1], Vicente Torres-Costa[1], Raul J. Martín-Palma[1], Pilar Herrero-Fernández[2], Miguel Angel García[3], Kazuhiro Fukami [4], Yukio H. Ogata [4], Miguel Manso Silván*[1]

[1]Departamento de Física Aplicada, Facultad de Ciencias, Universidad Autónoma de Madrid, 28049 Madrid, Spain.

[2]Instituto de Ciencia de Materiales de Madrid, Consejo Superior de Investigaciones Científicas, 28049 Madrid, Spain.

[3]Instituto de Cerámica y Vidrio, Consejo Superior de Investigaciones Científicas, 28049 Madrid, Spain.

[4] Institute of Advanced Energy, Kyoto University, Uji, Kyoto 611-0011, Japan.

*corresponding author: miguel.manso@uam.es, Tel:+34 914974918, Fax:+34 914973969

Abstract

Au films have recently increased their technological significance in view of the emerging electrical and optical applications. In this work we present a study on the preparation of nanoworm Au films onto Si (100) by the formation of an intermediate columnar porous silicon (PSi) layer. The films are resistant to peeling in different buffers and solvents. Adhesion arises from the presence of a diffused Au nucleation layer in the channeled PSi, which can be observed at short electroless Au deposition times. In longer experiments, an Au surface film grows from piled and aggregated Au crystals, which provide a high surface area. An X-ray absorption spectroscopy study reveals differences in the Au absorption edge that can be ascribed to the induced nanoroughness.

Keywords: gold nanostructures, electroless deposition, porous silicon, XTEM, STEM, XAS.

1. Introduction

Nanostructured Au films find relevant technological applications in several disciplines in view of its electrical, optical and surface properties, which are very frequently exploited simultaneously. Gold electrodes and contacts present good conductivities and relatively high oxidation potentials so that they are commonly used in analytical systems [1] and cellular stimulation protocols [2]. From the optical point of view, Au stands the reference material in reflectivity studies (especially in the IR but also in particular UV configurations) [3] and is prone to an intense surface plasmon resonance [4]. With regards to its surface properties, Au(111) terraces are the most referenced solid surface for the study of thiol based molecular monolayers [5]. Though large ordered domains of monolayers are only obtained when gold is deposited on mica substrates, a significant technological interest emerges from the deposition of gold on alternative transparent [6] or semiconductor substrates [7]. Deposition on Si(100), the reference microelectronics substrate, implies the growth of intermediate adhesive layer of Ti or Cr to avoid a tensile mismatch induced peeling. Identical requirement is necessary for the deposition of Au onto silica glass [8].

The use of Au in the form of nanoparticles allows to simultaneously exploit the plasmonic response [9] in gold and to follow the modification of such response by forming a diversity of complexes by thiol chemistry [10]. However, there is an increasing interest in the integration of the plasmonic properties of nanoparticles into solid substrates with the aim of defining new plasmonic configurations and the added value of increased surface area [11].

In the present work, we aim at making first approximation to the formation of high surface area Au structures onto silicon. We use as interface buffer layer a columnar film of porous silicon (PSi). Such a material has been already studied as matrix or template material of other metals [12] and oxides [13] and presents also relevant optical properties in view of the possibility to control the effective refractive index (i.e. by tailoring its porosity) and to emit visible light after UV excitation (i.e. quantum-crystal derived photoluminescence).

2. Experimental

2.1 Preparation of PSi

Porous silicon layers was obtained from high conductivity (0.01-0.02 Ωcm), p-type, silicon wafers. The anodization in 1:2 (volume) HF: Ethanol solutions (from commercial HF 48% (w/v) in water, Sigma-Aldrich) was carried out in a homemade Teflon® electrochemical cell, with a Pt reference electrode. Different current densities were set for obtain different porosities from 40 to 120 mA/cm^2 and a fixed etching time of 150 s for all of them was chosen. After etching, the Si/PSi substrates were rinsed in ethanol and dried with N_2.

2.2 Electroless Au deposition

Au deposition is carried out by displacement reaction from a precursor solution based on previous method [14]. Solution included 20 mM $HAuCl_4$, 200 mM HF and 20 mM NH_4OH was prepared in ultrapure water. All the reaction was carried out in the dark to avoid light-enhanced displacement reaction by the Si substrate. Precursor solution drops were placed over fresh and rinsed PSi substrates, and deposition time was controlled. Both substrate and film were immersed into 1:1 water:ethanol solution to remove solution and the rinsed twice with ethanol and twice with water. Au films were grown onto PSi for different deposition times (ta= 2, tb= 8 and tc= 32 min) and different porosities of the PSi matrix (labeled in the text according to anodization current; 120, 100, 80, 60 and 40 mA/cm^2, i.e. Au100SiP). Deposition time was fixed in 8 min for these latter conditions.

2.3 Characterization

XRD measurements were performed in a X`Pert PRO- Panalytical, with a graphite secondary monochromator. Cu Kα radiation was used in θ/2θ configuration obtaining diffractograms in the

10º-90º range with a step of 0.02º and 5 s integration time. FESEM images were acquired in a XL-30S FEG (PHILIPS). SEM images were obtained in a Hitachi S-3000N equipped with an EDX analyzer (Incax-sight, Oxford Instruments). TEM analysis were carried out in a JEOL JEM4000 (400 KV) provided with an STEM module which is sensitive in Z. Samples for cross section observation were prepared according to previously optimized protocols for mechanical and ion bean milling [15].

X ray absorption spectroscopy- (XAS) synchrotron experiments were carried in the L_3 edge of Au (2p3/2→5d5/2, 6s1/2, dipolar electronic transitions) at line BM25A of Spline in the European Synchrotron Radiation Facility (Grenoble, France). Both x-ray absorption near-edge structure (XANES) and extended x-ray absorption fine structure (EXAFS) spectra were obtained for each sample. The working energy from the colliding ring was 6 MeV. For the data treatment, software Athena [16] was used.

3. Results

3.1 Preliminary studies on Au/PSi

An initial study on the growth of Au films onto PSi columnar layers with different porosities was performed. To obtain homogeneous films with golden reflection, long deposition times were used, over 10 min. Equivalent films of circa 100 nm thickness were studied by XRD. The corresponding diffractograms are presented in figure 1. From their general shape it can be derived that all Au films obtained under different PSi porosities were polycrystalline with characteristic main diffraction peak at circa 42º corresponding to the 111 planes. Films grown on higher porosity structures presented a slight relative increase of the 111 planes with respect to those grown in low porosity PSi. Mean crystallite size estimated by the Scherrer formula [17] was also observed to be relatively higher for films grown on the more porous structures with respect to the low porosity PSi

films (circa 80 nm versus circa 70 nm, respectively). From these results, we could conclude that Au films obtained from PSi layers with highest porosity (Au120PSi) do not have a particular advantage with respect to those obtained at 100 mA/cm^2, which was defined as maximum porosity limit for the rest of the study.

The Au100PSi films were observed by SEM in cross section configuration as shown in figure 2. Figure 2a corresponds to a general view showing the characteristic columnar PSi obtained and the Au layer on top in a brighter contrast. An in depth composition analysis was performed by EDX in order to trace the presence of Au in the PSi layer (Figure 2b). The profile confirmed that Au structures were present in the PSi layer even at depths of almost 8 μm (i.e. down to the interface with the underlying Si). It could be also noted that there is a non negligible oxygen concentration in the mixed Au/PSi surfaces. A higher resolution image from the surface allows to better describe the Au film as a non dense, randomly woven filamentary structure (Fig 2c).

In order to evaluate Au film stability, the Au100PSi structures were immersed in different polar organic solvents and aqueous buffers. In particular, the films showed no signs of peeling for immersion in ethanol, toluene and PBS after 1 min soaking and ultrasound agitation.

3.2 First stages of Au nucleation into PSi.

The first stages of Au nucleation into de PSi matrix were studied by the preparation of cross section samples and observation by TEM. Figure 3.a shows a double cross section image of two facing columnar PSi substrates with deposited Au. From the magnification of the two facing surface in figure 3.b we can conclude that at short deposition times of 2 min a non negligible number of Au nanoclusters has already been formed on the surface of the PSi columnar pores. High resolution images (figure 3.c) allow confirming the crystalinity of these Au clusters with clear identification of interplanar distances of Au (111) planes (d= 0.2355 nm), which are even resolved locally in 2D forming crossing angles of 60º (see insert to figure 3.c). The Au crystals appear in a mesh of Si

crystalline structures, which are normally identified by Si (111) interplanar distances (d= 0.3135 nm). Other regions of the PSi matrix have suffered partial amorphization and oxidation so that the crystalline regions in PSi are reoriented with respect to the Si monocrystalline substrate (Fig. 3c). Observations in STEM mode were used in order to enhance the contrast arising from different Z for Si and Au. The infiltrated Au clusters create a clear diffusion profile with smaller and fewer clusters at increasing depth (Fig. 3d). However, in the deepest part of the PSi columns Au is still detected by EDX and it forms smaller nanoclusters of circa 5 nm (See inset in Fig. 3d).

3.3 XAS spectroscopy.

A XAS analysis was performed onto Au/PSi taking into account different porosities and deposition times. The spectra corresponding to Au100PSi grown for different deposition times (dominantly XANES region) are shown in figure 4a. The spectra show the typical profile of a polycrystalline gold film (see reference spectrum for Au foil). However, a slight modification can be observed in the absorption edge (see magnified region in the inset) with reduced intensity for deposited gold at the shorter periods. The EXAFS region of the spectra was used to determine by Fourier transformation the fine structure of the different gold structures. The radial distribution functions obtained are presented in figure 4b. All the spectra present identical general profile to the one obtained for the control Au foil. The differences in such functions leave very little chance to the presence of neighboring atoms different to Au even by considering the third neighbor.

Identical analysis was performed on AuPSi films with different substrate porosity. The spectra corresponding to Au films grown on PSi formed from 40 to 100 mA/cm^2 are presented in figure 5a. Again in this case the films show clear differences in the absorption edge intensity with respect to the Au foil reference. By increasing the porosity of the films the intensity was reduced and reduced porosity lead to closer intensity to the reference Au film (see magnification of the absorption edge in the inset). The use of the EXAFS region of the spectra to determine the radial

distribution functions led to an analog conclusion to that obtained previously. The similarity of all radial distribution functions leaves little place for considering, even at third order neighbors, the presence of alternative elements within the Au structures. However, in this case we can observe a slight shift towards smaller radius in the first neighbor maximum of the radial distribution function for the Au deposited layers with respect to the foil.

3. Discussion.

The process of gold electroless deposition in PSi can be categorized within displacement reactions according to the following chemical equation:

$$Au^{3+} + 3e^- \rightarrow Au$$

$$Si + 2H_2O \rightarrow SiO_2 + 4H^+ + 4e^-$$

Dissolved Au from $AuCl_4^-$ behaves as an oxidizing agent, while the PSi matrix takes the role of reducing agent, allowing the nucleation of metallic gold clusters. The complementary chemical equation for the PSi matrix is:

$$SiH_x + 2H_2O \rightarrow SiO_2 + (4+x)H^+ + (4+x)e^-$$

This reaction, in concomitance with the high potential for reduction of Au from $AuCl_4^-$, favors the formation of the Au clusters and the growth of the final Au film. A sequence of the previously presented results are in agreement with this interpretation for the Au nucleation reaction since they justify the presence of an independent Au metallic structure (i.e. XRD, TEM characterization) within an oxidized PSi matrix (i.e. oxygen in EDX analysis). In addition, for all times and porosities of the PSi matrix, we have obtained XAS spectra of Au L_3 absorption edge presenting similar characteristics to those for noble transition metals with fcc structure (first shoulder at 5 eV above the threshold is related to a full occupation of the d level) [18]. Changes in the intensity of this first peak can be interpreted in terms of size effects of the Au structures [19]. Deposited samples present small Au aggregates, which gain charge in the d level (i.e. loose d holes)

with respect to bulk Au due to a hybridation of s→d levels. In this sense, we observe in fact that the formation of Au in PSi would imply smaller Au structures at shorter times and high porosity of the matrix. An alternative interpretation to the scaled intensity patterns at the absorption edge could be attributed to the presence of an electronegative atom in the Au environment (S, O, Cl) [20]. However, the radial distribution functions leave only little chance to such structures. The slight differences in the first neighbor distances for the Au deposited films with respect to the Au foil is in agreement with a slight reduction in the first neighbor distance, though this is not confirmed by shifts in the XRD peaks.

Performing surface modification processes on Au surfaces for biomedical applications implies the use of certain adsorption/immobilization protocols. On the one hand, most of Au surface activation protocols are performed using thiol molecules, which are dissolved in Toluene solvents [21]. On the second hand, most protein (i.e. antibody-antigen and enzyme) adsorption assays are carried out in PBS [22]. Finally, ethanol immersion is a general sterilizing process in any cell culture experiment. It is important thus to outline herein that Au100PSi films withstand immersion conditions in all these media and can be thus considered for inclusion in many biomedical protocols.

5. Conclusions

Au films have been successfully deposited onto columnar PSi substrates of different porosity. Displacement reactions induce the formation of Au nanoworms on the PSi matrix at times as short as 2 min deposition. At longer times the clusters coalesce forming a mesh of filamentary structures on the PSi surface, which are resistant to ethanol, toluene and PBS immersion. The Au structures are crystalline and remain chemically independent of the SiO_x porous matrix formed from PSi during the deposition process. Shape arrangement is the most plausible explanation to the observation of lower intensity in the L_3 Au absorption edge with respect to Au foil reference.

Acknowledgments.

Authors would like to thank the ESRF for time allocation and financial support through experiment MA-1168. We also acknowledge funding provided by grant MAT2008-06858-C02-01 from Ministerio de Ciencia e Innovación (Spain), Madrid Regional Grant “Microseres” and financial resources from Fundación Domingo Martínez. The technical support from L García Pelayo is greatly appreciated.

References

[1] Lei CX, Wang H, Shen GL, Yu RQ. Immobilization of enzymes on the nano-Au film modified glassy carbon electrode for the determination of hydrogen peroxide and glucose. Electroanalysis. 2004;16:736-40.

[2] Park JS, Park K, Moon HT, Woo DG, Yang HN, Park KH. Electrical Pulsed Stimulation of Surfaces Homogeneously Coated with Gold Nanoparticles to Induce Neurite Outgrowth of PC12 Cells. Langmuir. 2009;25:451-7.

[3] Gan SY, Hong YL, Xu XD, Liu Y, Zhou HJ, Huo TL, et al. Influence of binding layer on the reflective performance of a Au film in vacuum ultraviolet wavelength region. Applied Optics. 2007;46:8641-4.

[4] Kambhampati DK, Knoll W. Surface-plasmon optical techniques. Current Opinion in Colloid & Interface Science. 1999;4:273-80.

[5] Frisbie CD, Fritschfaules I, Wollman EW, Wrighton MS. PREPARATION AND CHARACTERIZATION OF REDOX ACTIVE MOLECULAR ASSEMBLIES ON MICROELECTRODE ARRAYS. Thin Solid Films. 1992;210:341-7.

[6] Serrano A, de la Fuente OR, Garcia MA. Extended and localized surface plasmons in annealed Au films on glass substrates. Journal of Applied Physics. 2010;108.

[7] Gamero M, Alonso C. Deposition of nanostructurated gold on n-doped silicon substrate by different electrochemical methods. Journal of Applied Electrochemistry. 2010;40:175-90.

[8] Sexton BA, Feltis BN, Davis TJ. Characterisation of gold surface plasmon resonance sensor substrates. Sensors and Actuators a-Physical. 2008;141:471-5.

[9] Jain PK, Huang X, El-Sayed IH, El-Sayad MA. Review of some interesting surface plasmon resonance-enhanced properties of noble metal nanoparticles and their applications to biosystems. Plasmonics. 2007;2:107-18.

[10] de la Fuente JM, Barrientos AG, Rojas TC, Rojo J, Canada J, Fernandez A, et al. Gold glyconanoparticles as water-soluble polyvalent models to study carbohydrate interactions. Angewandte Chemie-International Edition. 2001;40:2258-+.

[11] Zhu SL, Fu YQ, Hou JZ. Topical Review: Metallic Nanoparticles Array for Immunoassay. Journal of Computational and Theoretical Nanoscience. 2010;7:1855-69.

[12] Ogata YH, Kobayashi K, Motoyama M. Electrochemical metal deposition on silicon. Current Opinion in Solid State & Materials Science. 2006;10:163-72.

[13] Singh RG, Singh F, Sulania I, Kanjilal D, Sehrawat K, Agarwal V, et al. Electronic excitations induced modifications of structural and optical properties of ZnO-porous silicon nanocomposites. Nuclear Instruments & Methods in Physics Research Section B-Beam Interactions with Materials and Atoms. 2009;267:2399-402.

[14] Brito-Neto JGA, Kondo K, Hayase M. Porous gold structures templated by porous silicon. Journal of the Electrochemical Society. 2008;155:D78-D82.

[15] Silvan MM, Langlet M, Duart JMM, Herrero P. Preparation of interfaces for TEM cross-section observation. Nuclear Instruments & Methods in Physics Research Section B-Beam Interactions with Materials and Atoms. 2007;257:623-6.

[16] Ravel B, Newville M. ATHENA, ARTEMIS, HEPHAESTUS: data analysis for X-ray absorption spectroscopy using IFEFFIT. Journal of Synchrotron Radiation. 2005;12:537-41.

[17] Patterson AL. The Scherrer formula for x-ray particle size determination. Physical Review. 1939;56:978-82.

[18] Kuhn M, Sham TK. CHARGE REDISTRIBUTION AND ELECTRONIC BEHAVIOR IN A SERIES OF AU-CU ALLOYS. Physical Review B. 1994;49:1647-61.

[19] Zhang P, Sham TK. X-ray studies of the structure and electronic behavior of alkanethiolate-capped gold nanoparticles: The interplay of size and surface effects. Physical Review Letters. 2003;90.
[20] Crespo P, Litran R, Rojas TC, Multigner M, de la Fuente JM, Sanchez-Lopez JC, et al. Permanent magnetism, magnetic anisotropy, and hysteresis of thiol-capped gold nanoparticles. Physical Review Letters. 2004;93.
[21] Gilbertson JD, Vijayaraghavan G, Stevenson KJ, Chandler BD. Air and water free solid-phase synthesis of thiol stabilized Au nanoparticles with anchored, recyclable dendrimer templates. Langmuir. 2007;23:11239-45.
[22] Le Guevel X, Daum N, Schneider M. Synthesis and characterization of human transferrin-stabilized gold nanoclusters. Nanotechnology. 2011;22:7.

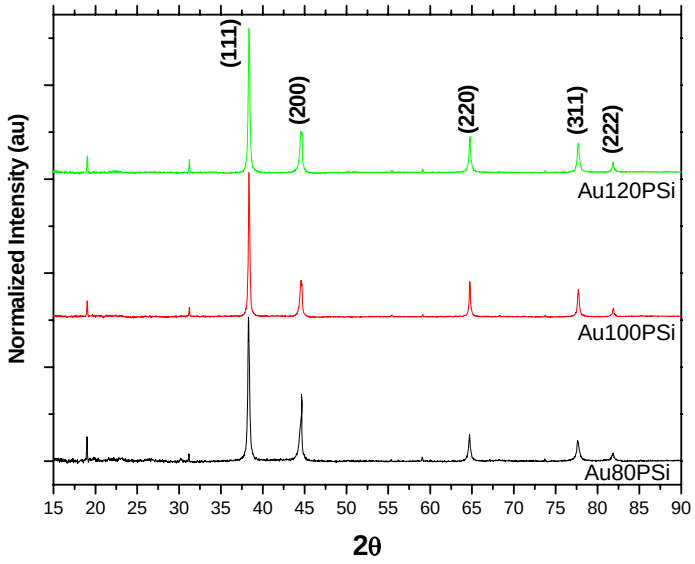

Figure 1. XRD diagrams of Au films grown on PSi layers formed at 80, 100 and 120 mA/cm^2 after deposition during 32 min.

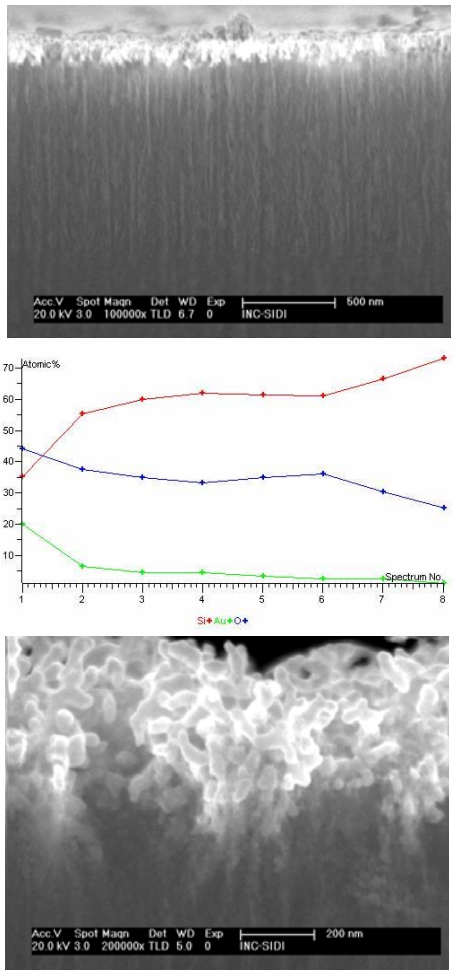

Figure 2. a) SEM image of the columnar PSi layer used as buffer and the top Au layer grown after deposition during 32 min. b) EDX in depth profile of the relative Au, Si and O composition (Au surface= point #1, silicon-PSi interface = point #8, 1 µm shift). c) Magnification from surface in a).

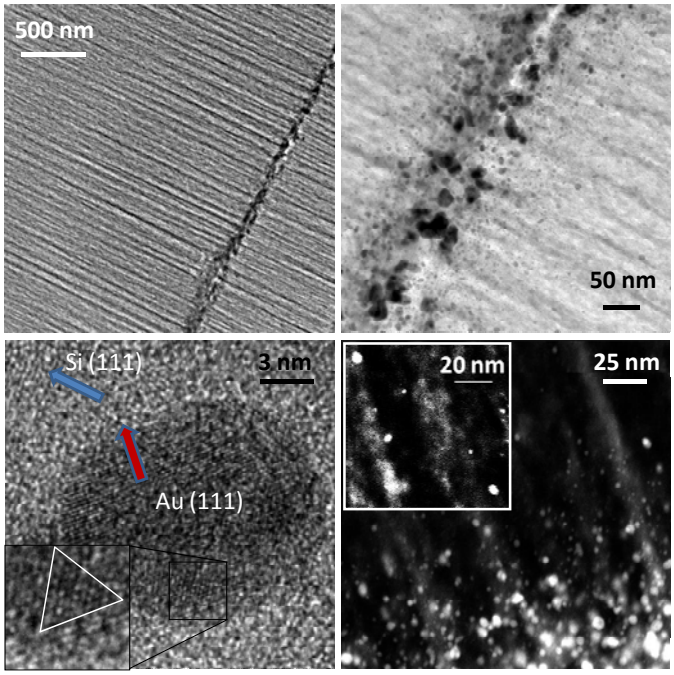

Figure 3. XTEM image of a sample prepared under short deposition times. STEM image showing the presence of Au clusters even at depths of various μm in the PSi.

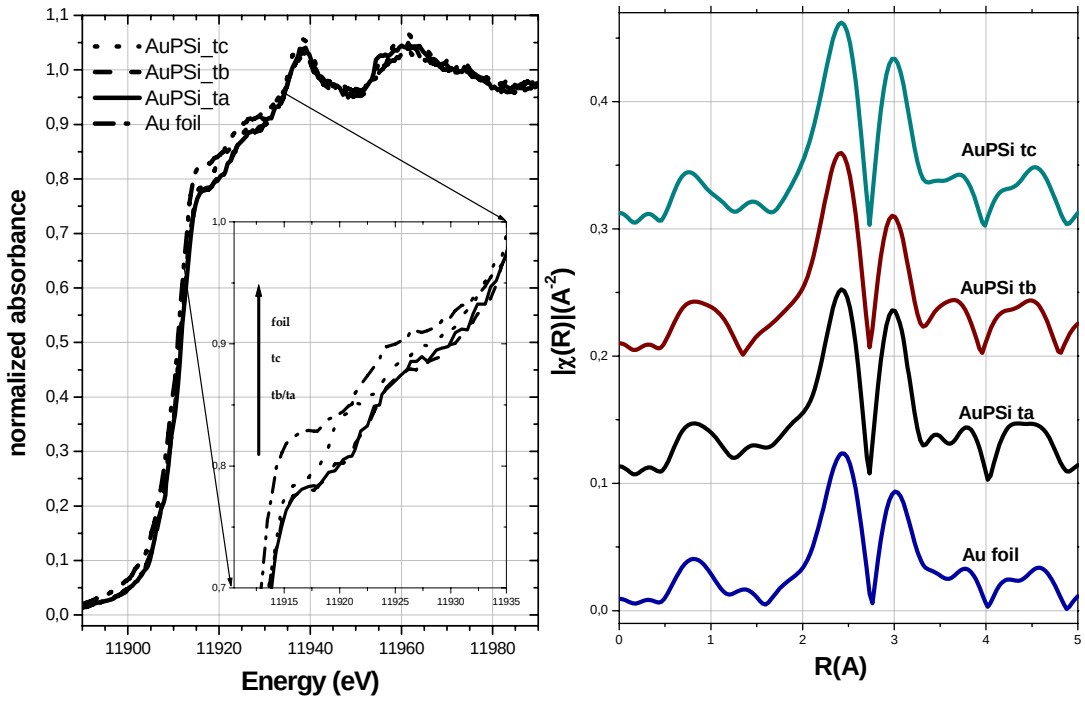

Figure 4. a) XAS spectra (EXAFS region) corresponding to Au100PSi films grown during different times along with an Au foil reference. b) Radial distribution functions obtained from the NEXAFS region of the Au100PSi films and the Au foil reference.

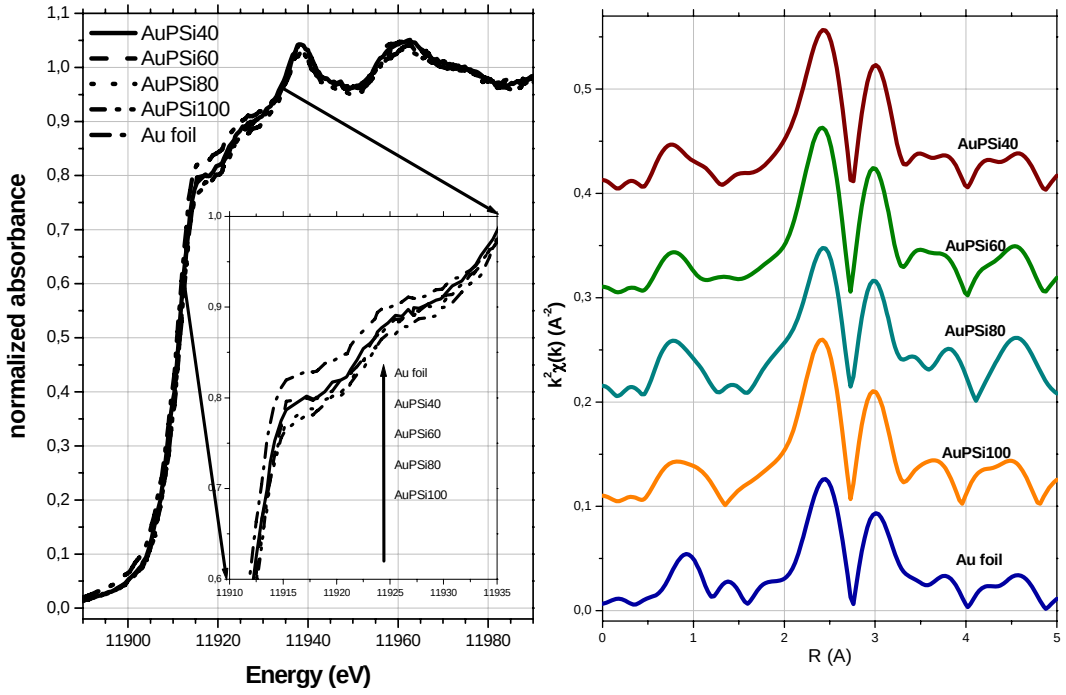

Figure 5. a) XAS spectra (EXAFS region) corresponding to Au films grown on PSi of different porosities during tb=8 min along with an Au foil reference. b) Radial distribution functions obtained from the NEXAFS region of the Au films on PSi of different porosity and from the Au foil reference.